ELSEVIER

Coordination Chemistry Reviews
200–202 (2000) 875–886

COORDINATION CHEMISTRY REVIEWS

www.elsevier.com/locate/ccr

Effects of driving force on the rates of intramolecular and bimolecular electron-transfer reactions

Harry B. Gray [a,*], Jay R. Winkler [a], David Wiedenfeld [b]

[a] *Beckman Institute, California Institute of Technology, Pasadena, CA 91125, USA*
[b] *Department of Chemistry, University of North Texas, Denton, TX 76203, USA*

Received 14 October 1999; accepted 7 January 2000

Contents

Abstract

Intramolecular electron transfer (ET) in $[Ir_2(\mu\text{-}pz^*)_2(CO)_2(Ph_2PO(CH_2)_2A^+)_2]$ $[B(Ph)_4^-]_2$ ($[IrPOpy^+]_2$; pz* = 3,5-dimethylpyrazolyl, A = pyridinium derivative, Ph = C_6H_5) exhibits a Gaussian free-energy dependence. The temperature dependences (200–280 K) of both excited-state ET ($Ir_2^* \rightarrow A^+$) and highly exergonic recombination ($A^\bullet \rightarrow Ir_2^\bullet$) reactions also agree remarkably well with semiclassical ET theory. Resonance Raman measurements on the *N*-ethyl-4-phenylpyridinium iodide charge-transfer complex reveal distortions along several vibrational modes upon pyridinium reduction. Neither semiclassical ET theory nor single-mode quantum theories can account quantitatively for all of the ET observations in $[IrPOpy^+]_2$. Bimolecular ET reactions between the triplet excited state of $[Ir(\mu\text{-}pz)(COD)]_2$ (pz = pyrazolyl, COD = 1,5-cyclooctadiene) and a series of *N*-alkylpyridinium acceptors

---

* Corresponding author. Tel.: +1-626-395 6500; fax: +1-626-449 4159.
E-mail address: hgcm@its.caltech.edu (H.B. Gray).

PII: S0010-8545(00)00261-7

remain limited by diffusion at driving forces where the recombination reactions are inverted.

Keywords: Electron transfer; Iridium; Pyridinium; Gaussian free-energy dependence

---

1. Introduction

Long-distance electron-transfer (ET) reactions are critical steps in photosynthesis and respiration. In photosynthesis [1], the excited-state ET step is followed by subsequent thermal transfers that increase the charge-separation distance and ultimately lead to photochemical energy storage; all steps leading to charge separation are faster than energy-wasting charge-recombination events. In order to design similarly efficient photochemical energy-storage systems, a thorough understanding of all factors governing ET rates is essential. Such knowledge could be employed as an aid in the construction of molecular electronics and artificial photosynthetic devices.

Semiclassical ET theory [2] (Eq. (1)) predicts that the rate constant (k_{ET}) for ET from a donor (D) to an acceptor (A) at fixed separation and orientation depends on the reaction driving force ($-\Delta G°$), a nuclear reorganization parameter (λ), and the electronic coupling strength between reactants and products at the transition state (H_{AB}). The reorganization energy, which reflects the change in equilibrium positions of nuclei before and after the reaction, is commonly separated into inner-sphere (λ_{I}) and solvent (λ_{S}) contributions. Rates are predicted to exhibit a Gaussian free-energy dependence, maximizing at $-\Delta G° = \lambda$; the region of increasing ET rates is commonly referred to as 'normal', while the region of falling ET rates is 'inverted'.

$$k_{\mathrm{ET}} = \sqrt{\frac{4\pi^3}{h^2 \lambda k_{\mathrm{B}} T}}\, H_{\mathrm{AB}}^2 \exp\left\{\frac{-(\Delta G° + \lambda)^2}{4\lambda k_{\mathrm{B}} T}\right\} \tag{1}$$

The bell-shaped free-energy dependence for k_{ET} has stimulated a great deal of experimental work. Early attempts to verify Eq. (1) involved measurements of the rates of excited-state ET (ET*) reactions. In an extensive study, Rehm and Weller found the expected increase in ET* rates at relatively low driving forces; however, the rates at high driving forces remained pegged at the diffusion limit [3]. Many other systems have exhibited analogous behavior [4].

In order to circumvent the diffusion limit, several research groups prepared molecules in which the electron donor and acceptor were incorporated into a single molecule [5–7]. Employing this strategy, Calcaterra et al. demonstrated inverted behavior in charge-shift reactions from a biphenylyl anion donor to a variety of electron acceptors linked by a rigid steroid spacer [5]. We also have employed this strategy to examine driving-force effects on ET in a series of complexes in which an Ir(I) dimer is covalently linked to substituted pyridinium acceptors [8].

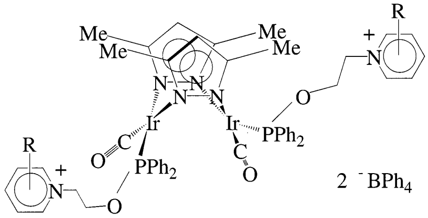

Fig. 1. The $[IrPOpy^+]_2$ electron donor–acceptor complexes. ET rate measurements were performed with complexes in which the pyridinium acceptors were unsubstituted, as well as in complexes with 4-methyl, 2,4,6-trimethyl, and 4-phenyl substituents on the heterocycle.

2. Intramolecular electron transfer

The composition of our electron donor–acceptor complexes is $[Ir_2(\mu\text{-}pz^*)_2(CO)_2(Ph_2PO(CH_2)_2A^+)_2][B(Ph)_4^-]_2$ ($[IrPOpy^+]_2$; pz* = 3,5-dimethylpyrazolyl, A = pyridinium derivative, Ph = C_6H_5; Fig. 1). ET driving force was varied by changing substituents on the pyridinium acceptors (A = unsubstituted, 4-methyl, 2,4,6-trimethyl, and 4-phenyl). An X-ray crystal structure determination of one of the complexes (A^+ = pyridinium) revealed a 5.8-Å separation between the closer Ir center and the N atom of the pyridinium ring [8b].

The range of driving forces that could be examined in $[IrPOpy^+]_2$ was constrained by the fact that phosphinite ligands could not be synthesized if the pyridinium group contained strongly electron-withdrawing substituents (e.g. nitriles). Measurements of excited-state reactions involving both singlet and triplet excited states of Ir_2 ($^1ET^*$ and $^3ET^*$), however, as well as the subsequent charge-recombination ET (^bET) processes (Fig. 2), gave rates that spanned nearly a 2.0-eV driving-force range.

Measurements on a model complex were necessary in order to extract ET rate constants from the overall rates of excited-state decay in $[IrPOpy^+]_2$; for this

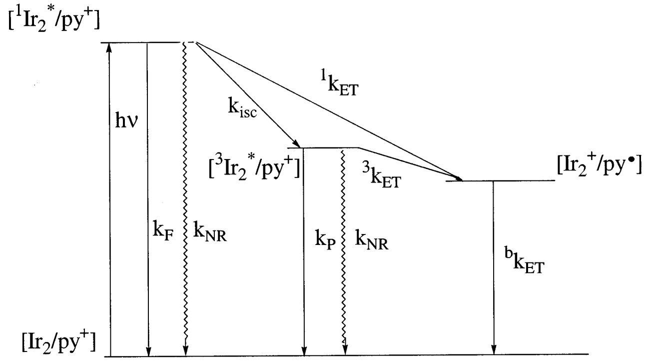

Fig. 2. Energy level diagram for the lowest-lying singlet ($^1Ir_2^*$) and triplet ($^3Ir_2^*$) excited states, and the charge-shift state of $[IrPOpy^+]_2$.

purpose a triethylammonium-based phosphinite ligand ($Ph_2PO(CH_2)_2N^+Et_3$) was incorporated into an Ir(I) complex. ^{1}ET*, ^{3}ET* and ^{b}ET rates in $[IrPOpy^+]_2$ were determined using luminescence-decay, transient-absorption, and fluorescence quantum-yield measurements. The free-energy changes associated with the ET reactions were estimated on the basis of electrochemical measurements on donor and acceptor groups, and the energies of the singlet and triplet excited states of the Ir(I) dimer.

A plot of the driving-force dependence of $[IrPOpy^+]_2$ ET* and ^{b}ET rates displays remarkably good agreement with semiclassical ET theory (Eq. (1); Fig. 3); the best fit to Eq. (1) yielded $\lambda = 1.06$ eV and $H_{AB} = 24$ cm^{-1}. The rates of ET* increase with driving force and maximize at 1.1×10^{11} s^{-1} near $-\Delta G° = 1$ eV. The ^{b}ET rates, however, decrease by two orders of magnitude as $-\Delta G°$ increases from 1.5 to 1.9 eV.

The observed Gaussian free-energy dependence for intramolecular ET within $[IrPOpy^+]_2$ suggests a minor role for nuclear tunneling. ET rates at high driving forces are deeply inverted, more so than would be expected if tunneling were important. This observation suggests that the inner-sphere contribution to the reorganization energy is relatively minor.

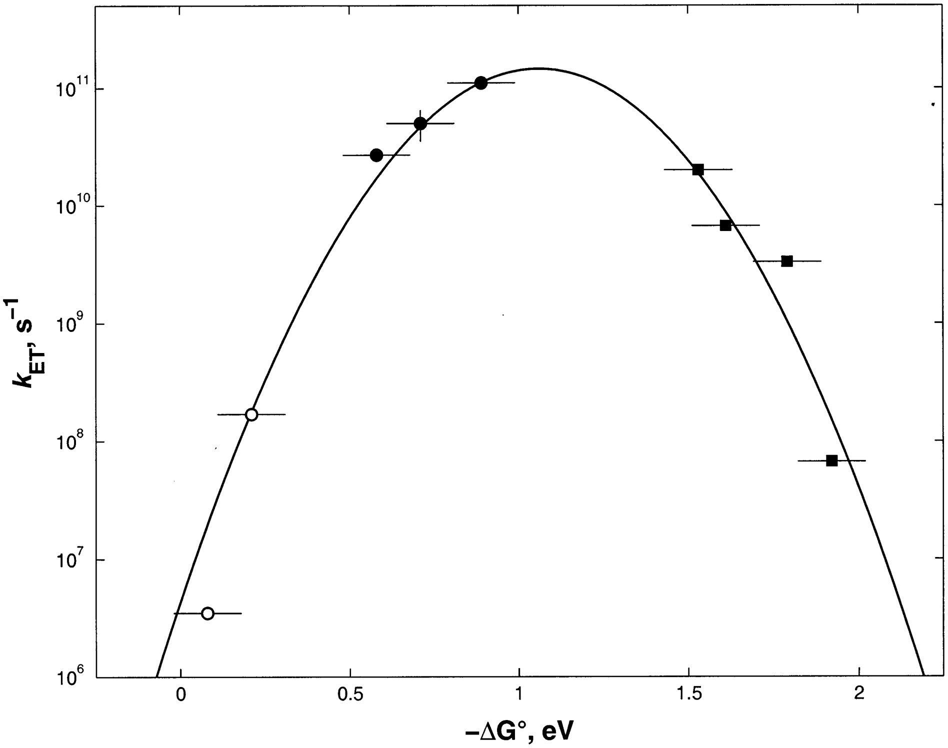

Fig. 3. Driving-force dependence of the $[IrPOpy^+]_2$ excited-state ($^1k^*_{ET}$, ●; $^3k^*_{ET}$, ○) and ground-state ($^bk_{ET}$, ■) ET rates; the solid line is a fit to Eq. (1) with $\lambda = 1.06$ eV and $H_{AB} = 24$ cm^{-1}.

In marked contrast, spectroscopic [9] and kinetics [5–7] measurements on organic donor–acceptor complexes suggest substantial inner-sphere distortions and important contributions from nuclear tunneling in the inverted region. In these systems, the driving-force dependences of ET rates are better described by quantum-mechanical ET models. Typically, a single-mode quantum rate expression [10] (Eq. (2), $S_f = \lambda_I/\hbar\omega$) is used: ET rates in the inverted region do not decrease as dramatically with increased driving force, owing to the effects of nuclear tunneling. The attenuated inverted effect found in organic donor–acceptor complexes stands in marked contrast to our results with $[\mathrm{IrPOpy}^+]_2$.

$$k_{\mathrm{ET}} = \sqrt{\frac{4\pi^3}{h^2\lambda_S k_B T}}\, H_{AB}^2 \exp(-S_f) \sum_{m=0}^{\infty} \frac{S_f^m}{m!} \exp\left\{\frac{-(\Delta G^\circ + \lambda_S + m\hbar\omega)^2}{4\lambda_S k_B T}\right\} \tag{2}$$

We pursued three distinct lines of inquiry to delineate the role of nuclear tunneling in the ET reactions of $[\mathrm{IrPOpy}^+]_2$: investigations of the temperature dependences of ET rates; studies of isotope effects on ET rates; and a spectroscopic evaluation of nuclear reorganization parameters [11].

2.1. Temperature effects

Previous investigations of organic donor–acceptor systems have shown that there is a weak or nonexistent temperature dependence of inverted ET rates; nuclear tunneling between nested reactant/product potential energy surfaces has been invoked to explain this phenomenon [12].

We examined $[\mathrm{IrPOpy}^+]_2$ ET* and ^{b}ET rates as functions of temperature in butyronitrile (Fig. 4). As was the case at room temperature, the driving-force dependences of ET rates at lower temperatures gave good fits to the semiclassical equation (Eq. (1)). The value of $\lambda = 1.04$ eV at 200 K did not change markedly with increasing temperature. Also consistent with the semiclassical theory, plots of $\ln(k_{\mathrm{ET}}T^{1/2})$ versus $1/T$ yielded straight lines with slopes whose absolute values decrease as $(\Delta G^\circ + \lambda)$ approaches zero. Importantly, the reaction rates varied with temperature in both the normal and inverted regions.

We did, however, note several discrepancies between the observed temperature dependences of $[\mathrm{IrPOpy}^+]_2$ ET rates and the predictions of the semiclassical model. First, the values of ΔH^* calculated using Eq. (1) deviated from those found experimentally. For the ET* reactions, the ΔH^* experimental values are all 0.05–0.1 eV greater than the theory predicts; the deviation is less systematic for the ^{b}ET reactions. Second, the apparent H_{AB} varies with temperature, increasing from 20 cm^{-1} at 200 K to 52 cm^{-1} at 280 K[1].

The dimethylene-based phosphinite spacer is not rigid and it is unlikely that a single conformation is adopted in solution. In related studies with peptide spacers, multiexponential kinetics were attributed to ET involving a mixture of conformers

---

[1] The difference in H_{AB} found for $[\mathrm{IrPOpy}^+]_2$ in acetonitrile as compared to butyronitrile is likely largely due to the flexibility of the dimethylene-based spacer. However, small solvent effects on H_{AB} have been reported even in rigidly linked systems (e.g. Ref. [6b]).

[13]. It is possible that the most favorable conformation for ET in $[IrPOpy^+]_2$ is not the most stable. The deviations from semiclassical theory could be due to the requirement that this favorable conformation must be formed prior to the ET event. To explain the observed driving-force dependences and first-order kinetics, it is necessary that the conformations exchange more rapidly than the electrons transfer. The barrierless deactivation in singlet-excited tetraphenylethylene (*TPE) at low temperature in butyronitrile provides a model for the conformational dynamics in $[IrPOpy^+]_2$. The deactivation pathway of *TPE involves a bond rotation limited largely by solvent viscosity. Our data indicate that the bond rotation in *TPE can occur very rapidly over the entire range of temperatures we used to study ET kinetics within $[IrPOpy^+]_2$.

A model in which ligand conformational changes are faster than ET in any of the conformers can explain our observations; in this case, formation of the reactive conformation(s) requires 0.05–0.1 eV. This model can account for: (1) the monoexponential nature of ET* and ^{b}ET kinetics in $[IrPOpy^+]_2$; (2) the increase in the apparent H_{AB} with increasing temperature; and (3) the deviation of observed activation energies from the predictions of semiclassical theory.

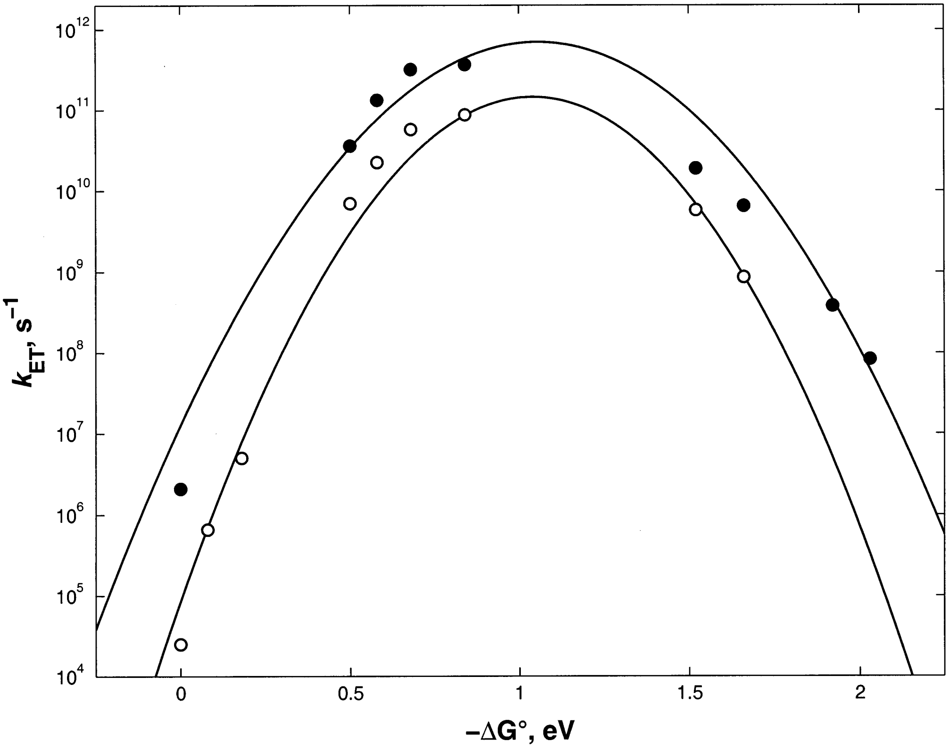

Fig. 4. Driving-force dependence of the $[IrPOpy^+]_2$ ET rates at 280 K (●) and 210 K (○) in butyronitrile. The solid lines are fits to Eq. (1) with the parameters: 280 K, $\lambda = 1.05$ eV and $H_{AB} = 52$ cm^{-1}; 210 K, $\lambda = 1.04$ eV and $H_{AB} = 22$ cm^{-1}.

2.2. Isotope effects

Kinetic isotope effects in ET reactions are usually interpreted in terms of nuclear tunneling [14]. We incorporated deuterated pyridine, 4-methylpyridine, and triethylamine into $[\mathrm{IrPOpy}^+]_2$ as a further probe of nuclear tunneling effects. The phosphinite ligands incorporating triethylamine serve as reference compounds (vide supra). In the complexes with deuterated pyridinium derivatives, rates for both normal and inverted reactions were slower than in natural abundance complexes. For example, k_H/k_D values are 1.18(9) and 1.43(8) for ^{1}ET* and ^{3}ET*, respectively, from Ir_2 to 4-methylpyridinium. Comparable isotope effects were found for the ^{1}ET* and ^{b}ET reactions with the unsubstituted pyridinium acceptor.

In contrast, no measurable isotope effect was found for excited-state decay in the triethylammonium model complex: $k_H/k_D = 1.02(2)$ at 200 K for triplet decay. These results unequivocally demonstrate the importance of isotope effects on the $[\mathrm{IrPOpy}^+]_2$ ET reactions. Furthermore, it is clear that the semiclassical model (Eq. (1)) cannot fully account for the observed kinetics.

2.3. Nuclear reorganization parameters

Charge-transfer absorption spectra along with the associated resonance Raman scattering spectra can provide independent information about nuclear rearrangements that accompany electron transfer [9,15]. We could not detect charge-transfer absorption in any of the $[\mathrm{IrPOpy}^+]_2$ complexes; this is consistent with our use of the nonadiabatic (weak-coupling) ET model, but did not allow us to obtain mode-specific information for any of the $[\mathrm{IrPOpy}^+]_2$ complexes.

Guided by previous studies [15], we chose the *N*-ethyl-4-phenylpyridinium iodide complex as a model for the pyridinium acceptors in the $[\mathrm{IrPOpy}^+]_2$ excited-state reactions. The Raman spectra of the iodide and chloride salts are shown in Fig. 5. It is clear that at least five modes are resonance-enhanced in the iodide-salt spectrum with the greatest enhancement in the 1565 cm^{-1} mode. This mode is believed to be associated with skeletal vibrations involving carbon–carbon bond stretching within the pyridinium ring. The enhanced Raman scattering from excitation in resonance with the charge-transfer absorption band is indicative of inner-sphere distortions associated with reduction of the pyridinium group. Clearly, the Raman spectra show that some inner-sphere distortion accompanies ET to an *N*-alkyl pyridinium group.

We used a single-quantum-mode rate expression (Eq. (2)) to estimate the inner-sphere and outer-sphere contributions to the reorganization energy. Fits to our data at any of the temperatures between 200 and 280 K consistently gave $\lambda_I < 0.04$ eV ($\hbar\omega = 1565\ \mathrm{cm}^{-1}$). As in the fits to the semiclassical equation, the value of λ_S (1.04 eV) did not change markedly with temperature[2].

---

[2] As found for the fit to Eq. (1), the value of H_{AB} increases with temperature (20 cm^{-1} at 200 K to 42 cm^{-1} at 280 K). This increase can be accounted for by $[\mathrm{IrPOpy}^+]_2$ conformational dynamics.

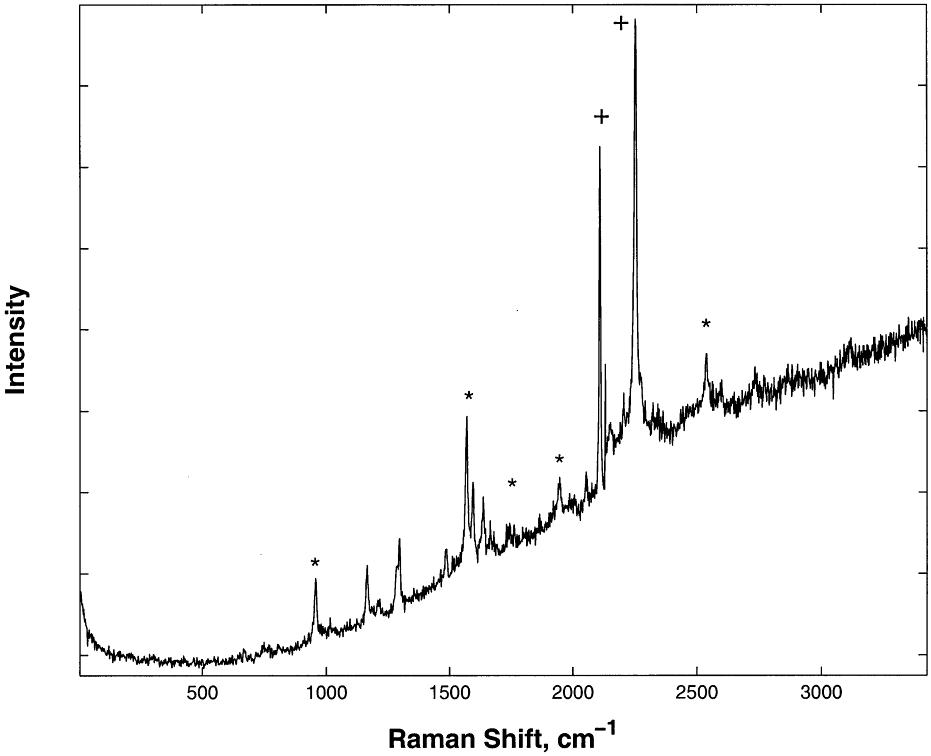

Fig. 5. Raman spectrum of the N-ethyl-4-phenylpyridinium iodide complex in CD_3CN (354.7 nm excitation). Resonance enhanced peaks are indicated by asterisks; solvent peaks are labeled with a plus sign.

Raman measurements were then made with deuterated derivatives of the 4-phenylpyridinium iodide complex: the frequency of the most intense resonantly enhanced peak shifts from 1565 to 1527 cm^{-1} on perdeuteration. These two frequency shifts were used with Eq. (2) to see if the observed $[IrPOpy^+]_2$ isotope effects could be reproduced. However, calculations (with $\lambda_S = 1.0$ eV and $\lambda_I = 0.04$ eV) over a wide driving-force range ($0 < -\Delta G^\circ < 1.5$ eV) at 200 K give k_H/k_D ratios that are not significantly different from unity. Clearly, the single-mode rate expression (Eq. (2)) cannot account for both the driving-force dependence and deuterium isotope effects of $[IrPOpy^+]_2$ ET.

We also have prepared $[IrPOpy^+]_2$ complexes with a different type of phosphinite ligand. The dimethylene bridge was replaced by a para-substituted-phenylene spacer bound directly or through methylenes to the pyridinium acceptor: $PPh_2O-(C_6H_4)-(CH_2)_n$-py$^+$ ($n = 0-3$) [16]. These ligands were synthesized to produce electron donor–acceptor complexes with greater conformational rigidity and to permit an examination of long-range couplings across the phenylene spacers.

ET kinetics were measured with three of the complexes incorporating phenylene spacers ($n = 1$–3). In one of the cases ($n = 2$), a minor reduction of the coupling strength compared to the dimethylene-based phosphinite spacer was observed. The $n = 1$ complexes gave a surprising result; the apparent electronic coupling for excited-state ET involving the Ir(I) triplet state was substantially smaller than that for the reactions of the singlet state. In a thorough theoretical study, Beratan and coworkers concluded that explicit treatment of conformational flexibility is important in analyzing the ET* data for the Ir(I) dimers with phenylene spacers [17].

3. Bimolecular electron transfer

Our early ET investigations using Ir(I) dimers focused on quenching the triplet excited state of $[\mathrm{Ir}(\mu\text{-pz})(\mathrm{COD})]_2$ (pz = pyrazolyl, COD = 1,5-cyclooctadiene) by a series of *N*-alkylpyridinium acceptors with widely varying reduction potentials [4]. The data could be well fit by the classical theory of outer-sphere ET. A plot of $RT \ln(k'_q)$ versus $E°$ $(\mathrm{A}^+/\mathrm{A})$ was found to be linear for pyridinium quenchers with values of $E°$ $(\mathrm{A}^+/\mathrm{A})$ greater than or approximately equal to $E°$ $(\mathrm{Ir}_2^+/{}^3\mathrm{Ir}_2^*)$; this corresponded to driving forces between 0.1 and 0.5 eV. At higher driving forces, the rates plateau at 10^{10} M^{-1} s^{-1}. This plateau of rates was unchanged at driving forces up to 1.18 eV.

Prompted by the observation of the inverted region in intramolecular $[\mathrm{IrPOpy}^+]_2$ ET reactions, we reinvestigated $[\mathrm{Ir}(\mu\text{-pz})(\mathrm{COD})]_2$ bimolecular ET with substituted *N*-alkylpyridinium acceptors that extended the driving force to 1.6 eV for excited-state ET [18]. The rates of ^{3}ET* reactions paralleled those measured in the prior study: rates increased monotonically and then remain pegged at the diffusion-limited rate starting at a driving force of about 1 eV. Strikingly, however, the ^{b}ET reactions (Fig. 6) exhibit inverted behavior for $-\Delta G° > 1.0$ eV.

One possible explanation for the absence of an inverted effect is that electronically excited products are formed in the highly exergonic ET* reactions [19,20]. Excited-state ET reactions typically involve closed-shell reactants with high-lying excited states. The products of ET* reactions, however, tend to be open-shell with low-lying excited states. Formation of excited products, sometimes accompanied by chemiluminescence, has long been recognized as a manifestation of the inverted effect. It is likely that, as a general rule, excited-state product formation will preclude direct observation of inverted effects in excited-state ET reactions. In the case of $[\mathrm{Ir}(\mu\text{-pz})(\mathrm{COD})]_2$ ^{3}ET* reactions, both the pyridinyl radical, and the Ir(I,II) dimer products are likely to have excited states at energies below 0.5 eV. The low energy and (expected) short lifetimes of these excited states will prevent direct observation of chemiluminescence. But, ET* reactions that form these excited products are predicted to be faster than the more exergonic processes that form ground-state products. Hence, the rates of ET* reactions do not decrease below the diffusion limit at high driving forces. Excited-product formation is not possible for the ^{b}ET reactions because the excited states of $[\mathrm{Ir}(\mu\text{-pz})(\mathrm{COD})]_2$ and *N*-alkylpyridinium groups are above 2 eV. Consequently, the ^{b}ET reactions display clear inverted behavior [21].

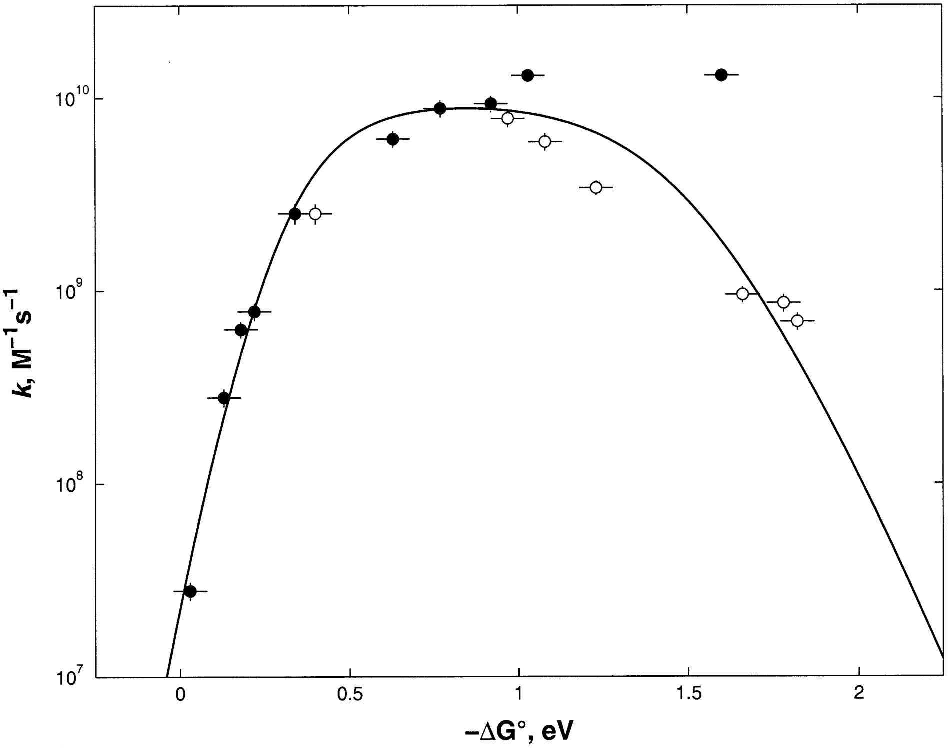

Fig. 6. Driving-force dependence of the rates of bimolecular ET from triplet excited [Ir(μ-pz)(COD)]$_2$ to *N*-alkylpyridinium acceptors (●) and the ground-state recombination reactions (○). The solid line was calculated using a steady-state model to describe formation of an encounter complex in which the electron transfer rate is given by Eq. (2) with the parameters: $S_r = 1.34$; $\hbar\omega = 1500$ cm^{-1}; $\lambda_S = 0.65$ eV; $H_{AB} = 12.5$ cm^{-1}. The diffusion-limited rate constant was assumed to be 1.2×10^{10} M^{-1} s^{-1}, and a value of 1 M^{-1} was used for the encounter-complex formation constant [18].

4. Concluding remarks

The most striking feature of the [IrPOpy$^+$]$_2$ ET kinetics is the strongly inverted free-energy dependence at high driving forces. The singlet photoinduced reactions are all between 5 and > 400 times faster than the corresponding recombination reactions at room temperature, although the latter processes all have driving forces greater by 0.5–1.5 eV. Maximizing both the photoinduced ET rate as well as the ratio of this rate to that of the energy-wasting recombination reaction are required to successfully mimic photosynthesis for solar energy storage. Therefore, it is important to understand how the Franck-Condon barrier to ET can be modulated. The inverted driving-force effects arise in the semiclassical formulation by an increase in the Franck-Condon barrier for ET as $-\Delta G°$ increases beyond the value of λ. Owing primarily to the effects of nuclear tunneling, the decrease in rate in the inverted region is attenuated when high-frequency ($\hbar\omega > 2k_BT$) modes associated with substantial inner-sphere distortions are coupled to the ET event. While we still do not possess a complete understanding of the ET reactions of $[IrPOpy^{+}]_2$, the isotope effect and resonance Raman studies indicate that nuclear tunneling does occur in this system. However, it seems clear that the rate constants in the deeply inverted region are not dominated by the distortions of high-frequency inner-sphere modes. The inverted effect can also be attenuated if low-energy electronic excited states can be formed; this would account for the observed bimolecular Ir(I) ET rate data in which recombination rates are highly inverted while photoinduced rates remain diffusion limited. Therefore, two strategies to maximize the inverted effect for ET rates are to use systems with electronically excited states well above the driving force of the reaction and to focus on reactions in which significant distortions of high-frequency inner-sphere modes are not dominant. Further understanding of how individual modes are coupled to ET processes will be required to implement the latter strategy.

Acknowledgements

Research at Caltech on the ET reactions of inorganic complexes is supported by the National Science Foundation (CHE-9610164). DW thanks the Robert A. Welch Foundation (Grant B-1415) for financial support at UNT.

References

[1] D.E. Budil, P. Gast, C.-H. Chang, M. Schiffer, J.R. Norris, Annu. Rev. Phys. Chem. 38 (1987) 561.

[2] R.A. Marcus, N. Sutin, Biochim. Biophys. Acta 811 (1985) 265.

[3] D. Rehm, A. Weller, Isr. J. Chem. 8 (1970) 259.

[4] J.L. Marshall, S.R. Stobart, H.B. Gray, J. Am. Chem. Soc. 106 (1984) 3027.

[5] (a) L.T. Calcaterra, G.L. Closs, J.R. Miller, J. Am. Chem. Soc. 105 (1983) 670. (b) G.L. Closs, J.R. Miller, Science 240 (1988) 440.

[6] (a) M.R. Wasielewski, M.P. Niemczyk, W.A. Svec, E.B. Pewitt, J. Am. Chem. Soc. 107 (1985) 1080. (b) A.D. Joran, B.A. Leland, P.M. Felker, A.H. Zewail, J.J. Hopfield, P.B. Dervan, Nature 327 (1987) 508. (c) M.R. Wasielewski, Chem. Rev. 92 (1992) 435. (d) P. Chen, R. Duesing, D.K. Graff, T.J. Meyer, J. Phys. Chem. 95 (1991) 5850.

[7] For bimolecular ET within organic ion pairs see: I.R. Gould, S. Farid, Acc. Chem. Res. 29 (1996) 522 and Refs. therein.

[8] (a) L.S. Fox, M. Kozik, J.R. Winkler, H.B. Gray, Science 247 (1990) 1069. (b) L.S. Fox, PhD Thesis, California Institute of Technology, Pasadena, 1989.

[9] A.B. Myers, Chem. Rev. (Washington, DC) 96 (1996) 911 and Refs. therein.

[10] B.S. Brunschwig, N. Sutin, Comments Inorg. Chem. 6 (1987) 209.

[11] D. Wiedenfeld, M. Bachrach, T.M. McCleskey, M.G. Hill, H.B. Gray, J.R. Winkler, J. Phys. Chem. B 101 (1997) 8823.

[12] (a) N. Liang, J.R. Miller, G.L. Closs, J. Am. Chem. Soc. 112 (1990) 5353. (b) J. Kroon, H. Oevering, J.W. Verhoeven, J.M. Warman, A.M. Oliver, M.N. Paddon-Row, J. Phys. Chem. 97 (1993) 5065. (c) A small temperature dependence of an inverted reaction has been reported (attributed to entropic effects and to changes in the distribution of solvent librations with temperature): P. Chen, S.L. Mecklenburg, T.J. Meyer, J. Phys. Chem. 97 (1993) 13126.

[13] (a) K.S. Schanze, K. Sauer, J. Am. Chem. Soc. 110 (1988) 1180. (b) S.S. Isied, M.Y. Ogawa, J.F. Wishart, Chem. Rev. (Washington, DC) 92 (1992) 381.

[14] (a) I.R. Gould, S. Farid, J. Am. Chem. Soc. 110 (1988) 7883. (b) R. Doolen, J.D. Simon, J. Am. Chem. Soc. 116 (1994) 1155.

[15] R.L. Blackbourn, C.S. Johnson, J.T. Hupp, M.A. Bryant, R.L. Sobocinski, J.E. Pemberton, J. Phys. Chem. 95 (1991) 10535.

[16] R.S. Farid, I.-J. Chang, J.R. Winkler, H.B. Gray, J. Phys. Chem. 98 (1994) 5176.

[17] I.V. Kurnikov, L.D. Zusman, M.G. Kurnikova, R.S. Farid, D.N. Beratan, J. Am. Chem. Soc. 119 (1997) 5690.

[18] (a) T.M. McCleskey, J.R. Winkler, H.B. Gray, J. Am. Chem. Soc. 114 (1992) 6935. (b) T.M. McCleskey, J.R. Winkler, H.B. Gray, Inorg. Chim. Acta 225 (1994) 319.

[19] Only modest inverted effects have been observed for bimolecular ET* reactions: (a) J.-M. Chen, T.-I. Ho, C.-Y. Mou, J. Phys. Chem. 94 (1990) 2889. (b) K.C. Cho, C.M. Che, K.M. Ng, C.L. Choy, J. Phys. Chem. 91 (1987) 3690. (c) K.C. Cho, C.M. Che, K.M. Ng, C.L. Choy, J. Am. Chem. Soc. 108 (1986) 2814. (d) C. Creutz, N. Sutin, J. Am. Chem. Soc. 99 (1977) 24.

[20] (a) K. Kikuchi, T. Niwa, Y. Takahashi, H. Ikeda, T. Miyashi, J. Phys. Chem. 97 (1993) 5070. (b) See also: G. Grampp, Angew. Chem. Int. Ed. Engl. 32 (1993) 691.

[21] In the intersecting-state model, the different $G°$ dependences of ET* and thermal ET reactions are ascribed to differences in the tightness of the transition states: (a) S.J. Formosinho, L.G. Arnaut, R. Fausto, Prog. React. Kinet. 23 (1998) 1. (b) S.J. Formosinho, L.G. Arnaut, J. Photochem. Photobiol. A: Chem. 82 (1994) 11.